

# Encapsulation of Fullerenes in a Helical PMMA Cavity Leading to a Robust Processable Complex with a Macromolecular Helicity Memory\*\*

Takehiro Kawauchi,\* Jiro Kumaki,\* Atsushi Kitaura, Kento Okoshi, Hiroshi Kusanagi, Keita Kobayashi, Toshiki Sugai, Hisanori Shinohara, and Eiji Yashima\*

The control and fabrication of the molecular ordering of fullerenes has attracted considerable attention because of their possible applications in advanced materials such as electronic and optoelectronic materials.<sup>[1]</sup> The supramolecular approach based on the self-assembly of functionalized fullerenes<sup>[2]</sup> or trapping of fullerenes by host molecules through inclusion<sup>[3]</sup> has been widely applied to make low-dimensional nanostructures of fullerenes with a rather high polydispersity. The uniform 1D alignment of fullerenes can be attained within carbon nanotubes (CNTs), which encapsulate fullerenes to form so-called fullerene “nanopeapods”.<sup>[4,5]</sup> The unique structural characteristics of fullerene nanopeapods provide intriguing chemical and physical properties,<sup>[5]</sup> but also make them difficult to synthesize and process. Fullerene-containing polymers may have a great potential for practical purposes owing to their easy processability, high mechanical strength, and availability of the polymers,<sup>[6]</sup> but there is no clear-cut strategy for controlling the distinct arrays of the

fullerenes in such systems. Herein, we report that syndiotactic poly(methyl methacrylate) (st-PMMA), a commodity plastic, encapsulates fullerenes such as C<sub>60</sub>, C<sub>70</sub>, and C<sub>84</sub> within its helical cavity to form a peapod-like crystalline complex that can be readily transformed into a homogeneous film. We also found that an optically active alcohol induces a preferred-handed helicity in the st-PMMA, whose helical conformation is “memorized”<sup>[7]</sup> after complete removal of the chiral alcohol and enforced by the inclusion of fullerenes in the st-PMMA helical cavity.

Syndiotactic PMMA has been reported to form a thermoreversible physical gel in aromatic solvents such as toluene, in which the st-PMMA chains adopt a helix of 74 units per 4 turns (74/4 helix) with a sufficiently large cavity of about 1 nm, and hence, solvents are encapsulated in the cavity of the inner helix.<sup>[8]</sup> We anticipated that fullerenes of specific sizes might be encapsulated in the helical cavity of the st-PMMA helices to form 1D regulated fullerene arrays (Figure 1 a).

To this end, st-PMMA (10 mg)<sup>[9]</sup> was dissolved in a toluene solution of C<sub>60</sub> (1 mg mL<sup>-1</sup>, 1 mL) upon heating at 110 °C. The solution was allowed to cool to room temperature,

[\*] Dr. T. Kawauchi,<sup>[†]</sup> Dr. J. Kumaki, Dr. K. Okoshi, Dr. H. Kusanagi, Prof. E. Yashima  
Yashima Super-structured Helix Project  
Exploratory Research for Advanced Technology (ERATO)  
Japan Science & Technology Agency (JST)  
101 Creation Core Nagoya, Shimoshidami, Moriyama-ku  
Nagoya 463-0003 (Japan)  
Fax: (+81) 52-739-2084  
E-mail: kawauchi@tutms.tut.ac.jp  
kumaki@yp-jst.jp  
yashima@apchem.nagoya-u.ac.jp

A. Kitaura, Prof. E. Yashima  
Department of Molecular Design and Engineering  
Graduate School of Engineering  
Nagoya University  
Chikusa-ku, Nagoya 464-8603 (Japan)  
Fax: (+81) 52-789-3185  
Homepage: <http://helix.mol.nagoya-u.ac.jp/>

K. Kobayashi, Dr. T. Sugai, Prof. H. Shinohara  
Department of Chemistry  
Graduate School of Science  
Nagoya University  
Chikusa-ku, Nagoya 464-8602 (Japan)

[†] Present address: School of Materials Science  
Toyoashi University of Technology  
Tempaku-cho, Toyoashi 441-8580 (Japan)

[\*\*] We are deeply grateful to Prof. N. Tanaka, Prof. M. M. Green, and Prof. Y. Okamoto for valuable discussions. PMMA = poly(methyl methacrylate).

Supporting information for this article is available on the WWW under <http://www.angewandte.org> or from the author.

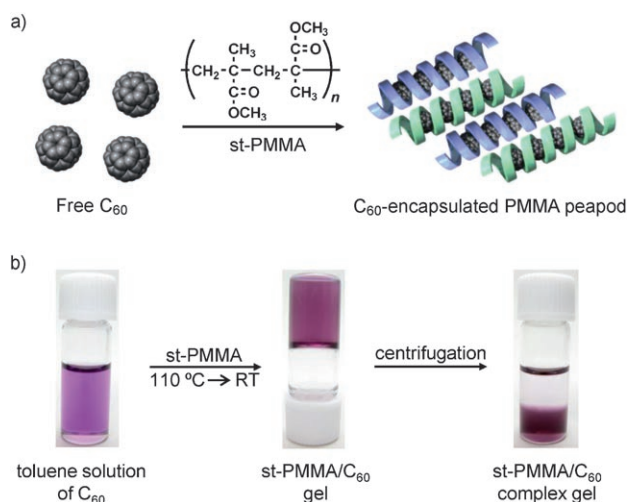


**Figure 1.** a) Schematic illustration of the encapsulation of C<sub>60</sub> in the st-PMMA helical cavity upon gelation. Right- (blue) and left-handed (green) helical complexes are equally produced. b) Photographs of a toluene solution of C<sub>60</sub> (1 mg mL<sup>-1</sup>, 1 mL; left), st-PMMA/C<sub>60</sub> gel after the addition of st-PMMA (10 mg) with subsequent heating to 110 °C and then cooling to room temperature (middle), and st-PMMA/C<sub>60</sub> complex gel after centrifugation at 1700 g for 10 min (right).

and it gelled within a few minutes. After centrifugation, we obtained a purple-colored condensed gel, while the supernatant became pale pink (Figure 1b). The electronic absorption spectra of the feed  $C_{60}$  solution and the supernatant indicate that 0.91 mg of  $C_{60}$  (8.3 wt %) was encapsulated in the st-PMMA cavities. The encapsulated  $C_{60}$  content increased with increasing feed  $C_{60}$  concentration and reached a maximum amount of 1.3 mg in toluene (Table S1 in the Supporting Information). When 1,2-dichlorobenzene (DCB), a better solvent for solubilizing  $C_{60}$ , was used as the cosolvent (50 vol % in toluene), the st-PMMA more efficiently trapped  $C_{60}$  (23.5 wt %, 3.1 mg per 10 mg of st-PMMA; Table S1 in the Supporting Information; for the effect of the DCB amounts on the encapsulation of  $C_{60}$  in toluene, see Figure S1 in the Supporting Information), and the amount of the st-PMMA helical hollow space that is filled with  $C_{60}$  molecules is roughly estimated to be 86 % based on a possible helical structure of st-PMMA filled with  $C_{60}$  in a 1D close-packing manner (see below and Table S1 in the Supporting Information).

We then investigated the thermal stabilities of the st-PMMA and st-PMMA/ $C_{60}$  gels by measuring their melting behavior using  $^1\text{H}$  NMR spectroscopy.<sup>[10]</sup> A st-PMMA gel started melting at around 40 °C, while the st-PMMA/ $C_{60}$  gel maintained its gel structure over 60 °C resulting from encapsulation of the  $C_{60}$  molecules within the helical cavity of st-PMMA, thereby acting to reinforce the st-PMMA physical gel (Figure S2 and Table S1 in the Supporting Information). Differential scanning calorimetry (DSC) and X-ray diffraction (XRD) profiles of the st-PMMA/ $C_{60}$  films with different  $C_{60}$  contents (11.7 and 23.5 wt %) revealed a crystalline structure of the st-PMMA/ $C_{60}$  complex (Figure 2) that is essentially different from that of the st-PMMA film. The st-PMMA/ $C_{60}$  film containing 23.5 wt % of  $C_{60}$  maintained the crystal structure after evaporation of the solvents and exhibited a birefringence as observed by polarizing optical microscopy (Figure 2k), whereas the st-PMMA film showed no birefringence (Figure 2j). We note that isotactic PMMA (it-PMMA) cannot encapsulate  $C_{60}$  molecules at all, and the  $C_{60}$  precipitated upon evaporating the solvent from an it-PMMA/ $C_{60}$  mixture in toluene in spite of the low  $C_{60}$  content (4.8 wt %; Figure S3 in the Supporting Information). The st-PMMA film showed only a heat capacity change at the glass-transition temperature ( $T_g = 126.7^\circ\text{C}$ ) as observed for typical amorphous st-PMMA (Figure 2a), indicating that a helical conformation induced in the st-PMMA chains in a gel formed in aromatic solvents is disrupted once the solvents are completely removed by evaporation, as supported by the broad XRD pattern (Figure 2e). In sharp contrast, the st-PMMA/ $C_{60}$  film con-

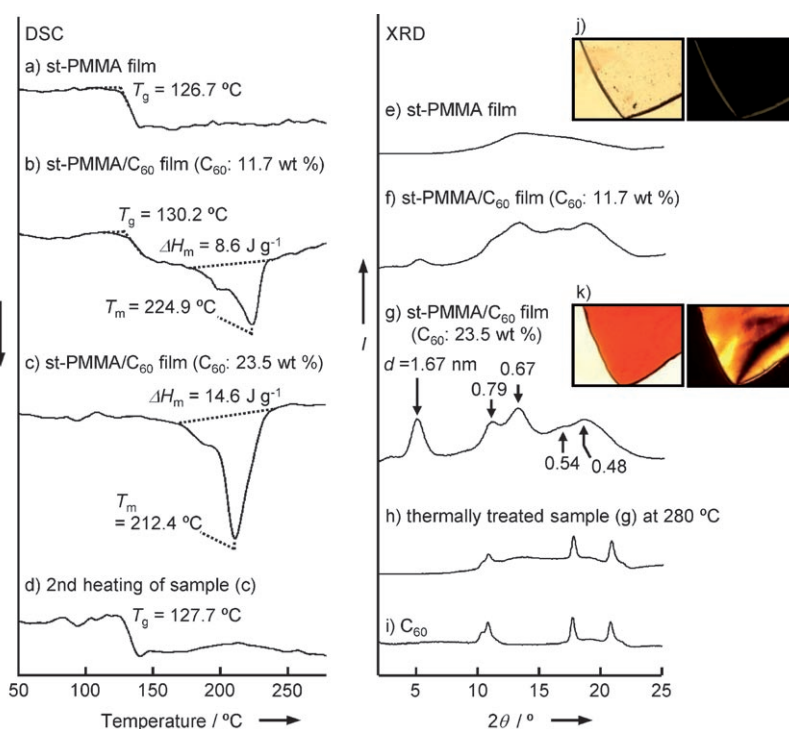


**Figure 2.** DSC thermograms of a) st-PMMA film and b, c) st-PMMA/ $C_{60}$  complex films containing 11.7 (b) and 23.5 wt % (c)  $C_{60}$ . These films were prepared by evaporating the solvents from the st-PMMA and st-PMMA/ $C_{60}$  complex gels in toluene or a toluene/DCB mixture (50 vol %), thus producing homogeneous films without any phase separation even at a high  $C_{60}$  content. The measurements were conducted after cooling the samples at 0 °C, followed by heating to 280 °C (10 °C min<sup>-1</sup>) under nitrogen. The sample (c) was then cooled to 0 °C (10 °C min<sup>-1</sup>), and then heated again (d; 10 °C min<sup>-1</sup>). The arrow to the left of the DSC data indicates the endothermic direction. e–i) XRD profiles of st-PMMA film (e), st-PMMA/ $C_{60}$  complex film (f; 11.7 wt %  $C_{60}$ ), st-PMMA/ $C_{60}$  complex film (23.5 wt %  $C_{60}$ ) before (g) and after (h) thermal treatment at 280 °C for 3 min, and bulk  $C_{60}$  (i). j, k) Polarized (right) and nonpolarized (left) optical micrographs of st-PMMA (j) and st-PMMA/ $C_{60}$  complex (k; 23.5 wt %  $C_{60}$ ) films. Dimensions of micrographs in (j) and (k): 1 × 1.3 mm<sup>2</sup>.

taining 11.7 wt % of  $C_{60}$  revealed an additional endothermic peak at 224.9 °C corresponding to the melting temperature ( $T_m$ ) of the st-PMMA/ $C_{60}$  complex (Figure 2b). Increasing the  $C_{60}$  content (23.5 wt %) brought about an increase in the crystallinity, and the melting peak increased, accompanied by the near disappearance of the  $T_g$  peak (Figure 2c). As a consequence, the st-PMMA helical hollow spaces may be filled with 23.5 wt %  $C_{60}$  molecules, which agrees approximately with the estimated filling ratio (86 %; Table S1 in the Supporting Information). Further strong evidence for the crystalline structure of the st-PMMA/ $C_{60}$  complex observed is its characteristic XRD pattern, which is completely different from those of the st-PMMA (Figure 2e) and  $C_{60}$  films (Figure 2i); the st-PMMA/ $C_{60}$  complex has an apparent  $d$  spacing of 1.67 nm (Figure 2f and g). Further heating of the st-PMMA/ $C_{60}$  film (23.5 wt %) at 280 °C, which is higher than  $T_m$ , gave rise to an irreversible release of the encapsulated  $C_{60}$  molecules, resulting in amorphous st-PMMA and  $C_{60}$  aggregates as supported by the DSC and XRD profiles (Figure 2d and h, respectively).

In the same way,  $C_{70}$  and  $C_{84}$  molecules can be encapsulated in the st-PMMA hollow spaces to form crystalline

condensed gels and films (Figures S4 and S5, respectively, in the Supporting Information). Interestingly, the  $d$ -spacing value observed by XRD increased with an increase in the size of the encapsulated fullerenes, from 1.67 ( $C_{60}$ ) to 1.92 ( $C_{70}$ ) and 2.04 nm ( $C_{84}$ ), indicating that the st-PMMA helical cavity likely expands upon encapsulation of the larger fullerenes, and this change may be accompanied by a change in the helical pitch of the st-PMMA.

Atomic force microscopy (AFM) of a st-PMMA/ $C_{60}$  Langmuir–Blodgett (LB) film deposited on mica afforded further evidence for the inclusion of  $C_{60}$  in the st-PMMA. The mixed monolayer of st-PMMA and  $C_{60}$ , spread on a water surface, formed a crystalline rodlike structure with a lamellar alignment upon compression (Figure 3a) whose surface pressure–area ( $\pi$ – $A$ ) isotherm was different from those of st-PMMA and  $C_{60}$  alone (Figure S6 in the Supporting Information). The AFM image revealed helix-bundle struc-

tures, which are further resolved into individual stripe-patterned chains with a chain–chain lateral spacing of  $(1.9 \pm 0.1)$  nm and a helical pitch of  $0.9 \pm 0.1$  nm. Transmission electron microscopy (TEM) of the LB film suggests a 1D alignment of  $C_{60}$  molecules (with an average intermolecular distance of about 1 nm), which may be encapsulated within the undetectable st-PMMA helices during irradiation with 120-keV electrons (Figure 3b, and Figure S7 in the Supporting Information).<sup>[11]</sup> Figure 3c shows a possible structure of the st-PMMA/ $C_{60}$  complex calculated on the basis of the reported helical structure of st-PMMA<sup>[8,12]</sup> (Figure S8 and Table S2 in the Supporting Information) in which the  $C_{60}$  molecules are encapsulated to form a regular 1D array with an intermolecular distance of 1.0 nm. The helical pitch and lateral spacing of the st-PMMA including the  $C_{60}$  molecules, estimated by AFM, are in good agreement with those of the proposed model. Molecular dynamics (MD) simulations revealed that the included  $C_{60}$  molecules remain within the helical cavity of the st-PMMA at 400 K for 200 ps, which supports its thermal stability (see the Supporting Information).

We also found that a preferred-handed helical st-PMMA can be formed by an optically active aromatic alcohol,<sup>[13]</sup> (*R*)- or (*S*)-1-phenylethanol (**1**), when used as the gelling medium during the st-PMMA/ $C_{60}$  gel formation (Figure 4a). Surprisingly, the induced form of the helix is retained after the optically active **1** is completely removed. The optically active st-PMMA/ $C_{60}$  complex gel was prepared in a similar way in [*D*<sub>8</sub>]toluene with (*R*)-**1** (20 vol %) and subsequent complete removal of the (*R*)-**1** by repeatedly washing the gel with [*D*<sub>8</sub>]toluene, and then isolated by centrifugation (Table S3 in the Supporting Information).<sup>[14]</sup> The gel without any trace amount of (*R*)-**1** exhibited a vibrational circular dichroism (VCD) in the PMMA IR regions owing to the helical structure of the st-PMMA with an excess of one handedness whose helicity is further “memorized” after removal of the (*R*)-**1** (Figure 4b). When (*S*)-**1** was used instead, st-PMMA with the opposite helicity was formed, as evidenced by the mirror-image VCD. We then calculated the IR and VCD spectra for the right- and left-handed helical 18/1 st-PMMA at the B3LYP/6-31G(d) level (Figure 4c, and Table S4 in the Supporting Information). The calculated spectra fit well to the observed spectra, suggesting that the st-PMMA helix induced by (*R*)-**1** is likely right handed.

Owing to a preferred-handed helical structure of the st-PMMA nanotube, we also observed an induced electronic CD (ECD) in the encapsulated  $C_{60}$  chromophore regions, although  $C_{60}$  itself is achiral (Figure 4d, and Figure S9 in the Supporting Information).<sup>[15,16]</sup> A weak but apparent bisignate ECD band at 656 nm also supports the encapsulation of the  $C_{60}$  molecules within the tubular cavity of the helical st-PMMA. The fact that the broad absorption band at around 450 nm only appears in the st-PMMA/ $C_{60}$  complex gel (Figure S10 in the Supporting Information) supports the stacking interactions between neighboring  $C_{60}$  molecules,<sup>[15,16]</sup> which may lead to a color change of the complex gel (Figure 1b). The encapsulation of  $C_{60}$  in the helical st-PMMA nanotube is essential for the induced ECD since a solution of st-PMMA and  $C_{60}$  in toluene with 30 vol % (*R*)-**1**

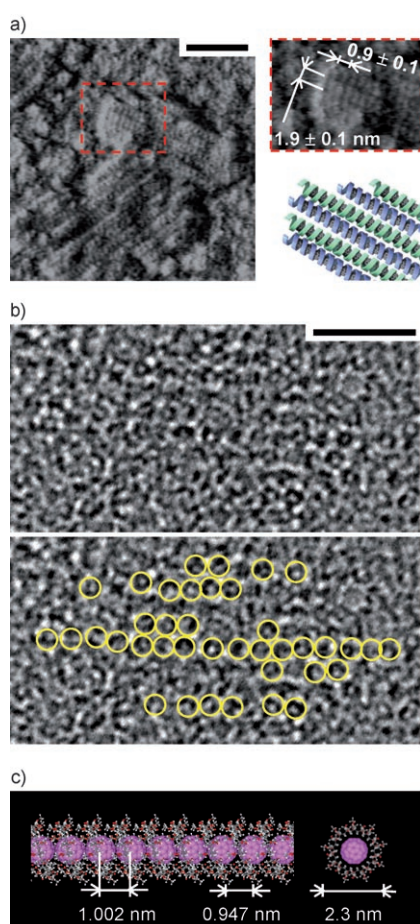


**Figure 3.** a) Left: Tapping-mode AFM phase image of an LB film of the st-PMMA/ $C_{60}$  complex deposited on mica; scale bar: 10 nm. Right: Magnified image of the area indicated by the dotted square (top) and schematic representation of a possible bundle structure of the helical st-PMMA/ $C_{60}$  complex (bottom). b) High-resolution TEM image of an LB film of the st-PMMA/ $C_{60}$  complex (top) and 1D alignment of the  $C_{60}$  molecules (bottom), indicated by the yellow circles (diameter: 1 nm);<sup>[11]</sup> scale bar: 5 nm. c) Energy-minimized structure of the st-PMMA/ $C_{60}$  complex: side view (left) and top view (right). A computational study was performed at the B3LYP/6-31(d) level under periodic boundary conditions (see the Supporting Information).



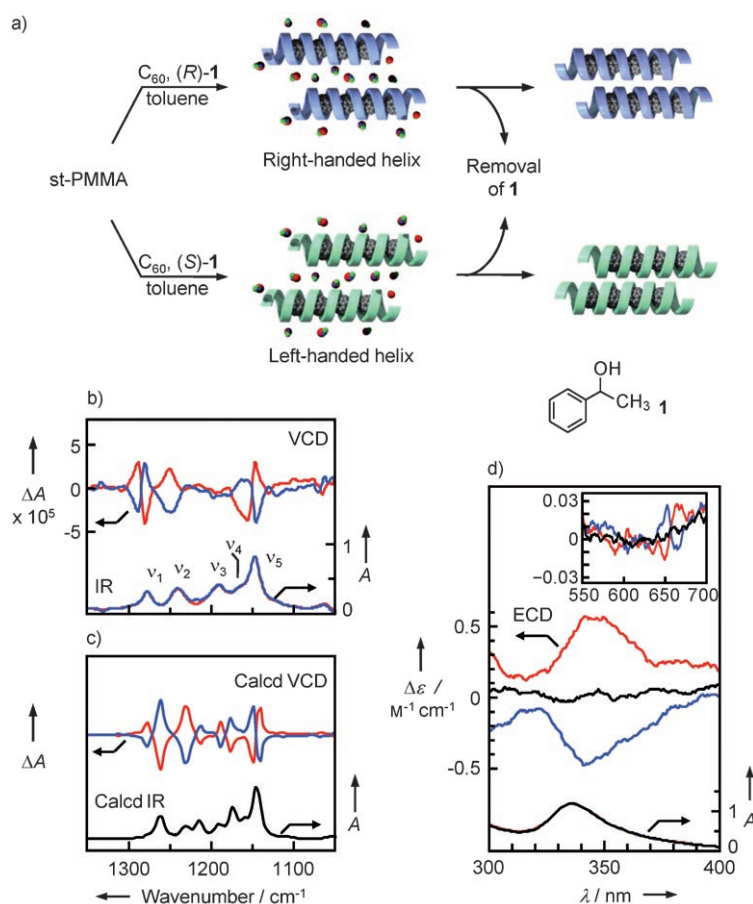


**Figure 4.** Optically active C<sub>60</sub>-encapsulated st-PMMA with macromolecular helicity memory. a) Schematic illustration of right- (top) and left-handed (bottom) helicity induction in the C<sub>60</sub>-encapsulated st-PMMA in the presence of (R)- or (S)-1. b) Observed VCD (top) and IR (bottom) spectra of isolated st-PMMA/C<sub>60</sub> complex gels (3.1 wt% C<sub>60</sub>) in [D<sub>8</sub>]toluene prepared by (R)-1 (red lines) and (S)-1 (blue lines), measured after the complete removal of 1. For the assignments of the experimental and calculated IR and VCD bands (v<sub>1</sub>–v<sub>5</sub>), see Table S4 in the Supporting Information. The x axis is the same as in (c). c) Calculated VCD (top) and IR (bottom) spectra of right- (red line) and left-handed (blue line) helical st-PMMA. d) Observed ECD (top) and absorption (bottom) spectra of isolated st-PMMA/C<sub>60</sub> complex gels in toluene prepared by racemic 1 (black lines), (R)-1 (red lines), and (S)-1 (blue lines). The inset shows the corresponding ECD spectra in the long-wavelength regions (for the corresponding absorption spectra, see Figure S9 in the Supporting Information). The contribution of the linear dichroism caused by the macroscopic anisotropy was negligible.

does not turn into a gel and exhibits no ECD at all. The optically active st-PMMA/C<sub>60</sub> complex gel and film are thermally stable up to their melting temperatures. In the absence of C<sub>60</sub>, a similar optically active st-PMMA gel can be prepared with (R)- or (S)-1 in toluene. The induced st-PMMA helix also remains after complete removal of the optically active 1, and this helical st-PMMA can serve as a template for the further inclusion of C<sub>60</sub> molecules, resulting in a st-PMMA/C<sub>60</sub> complex gel, thus showing virtually the same VCD and ECD spectra as shown in Figure 4 (see Figure S11 in the Supporting Information).

The results reported here show that st-PMMA can encapsulate fullerenes to mimic to some extent the behavior

of CNTs. Unlike the latter, the fullerene-encapsulated st-PMMA is easy to prepare, inexpensive, and processable. Moreover, its helical sense can be controlled to produce an optically active supramolecular peapod. These unique supramolecular helical complexes offer potentially useful chiral materials as well as optoelectronic materials.

Received: August 10, 2007

Published online: November 30, 2007

**Keywords:** chiral memory · fullerenes · helical structures · nanotubes · supramolecular chemistry

- [1] a) K. M. Kadish, R. S. Ruoff in *Fullerenes: Chemistry, Physics, and Technology*, Wiley-Interscience, New York, **2000**; b) M. Prato, *J. Mater. Chem.* **1997**, 7, 1097–1109; c) Y. Chen, Z. Huang, R. F. Cai, B. C. Yu, *Eur. Polym. J.* **1998**, 34, 137–151; d) M. Prato, M. Maggini, *Acc. Chem. Res.* **1998**, 31, 519–526; e) A. Cravino, N. S. Sariciftci, *J. Mater. Chem.* **2002**, 12, 1931–1943; f) S. Fukuzumi, *Bull. Chem. Soc. Jpn.* **2006**, 79, 177–195.
- [2] a) E. Nakamura, H. Isobe, *Acc. Chem. Res.* **2003**, 36, 807–815; b) D. M. Guldi, F. Zerbetto, V. Georgakilas, M. Prato, *Acc. Chem. Res.* **2005**, 38, 38–43.
- [3] a) F. Diederich, M. G. López, *Chem. Soc. Rev.* **1999**, 28, 263–277; b) P. D. W. Boyd, C. A. Reed, *Acc. Chem. Res.* **2005**, 38, 235–242; c) K. Tashiro, T. Aida, *Chem. Soc. Rev.* **2007**, 36, 189–197.
- [4] a) B. W. Smith, M. Monthieux, D. E. Luzzi, *Nature* **1998**, 396, 323–324; b) K. Hirahara, K. Suenaga, S. Bandow, H. Kato, T. Okazaki, H. Shinohara, S. Iijima, *Phys. Rev. Lett.* **2000**, 85, 5384–5387.
- [5] a) J. Sloan, A. I. Kirkland, J. L. Hutchison, M. L. H. Green, *Chem. Commun.* **2002**, 1319–1332; b) O. Vostrowsky, A. Hirsch, *Angew. Chem.* **2004**, 116, 2380–2383; *Angew. Chem. Int. Ed.* **2004**, 43, 2326–2329; c) A. N. Khlobystov, D. A. Britz, G. A. D. Briggs, *Acc. Chem. Res.* **2005**, 38, 901–909; d) R. Kitaura, H. Shinohara, *Chem. Asian J.* **2006**, 1, 646–655.
- [6] a) C. Wang, Z.-X. Guo, S. Fu, W. Wu, D. Zhu, *Prog. Polym. Sci.* **2004**, 29, 1079–1141; b) F. Giacalone, N. Martin, *Chem. Rev.* **2006**, 106, 5136–5190; c) Z. T. Ball, K. Sivula, J. M. J. Fréchet, *Macromolecules* **2006**, 39, 70–72.
- [7] a) E. Yashima, K. Maeda, Y. Okamoto, *Nature* **1999**, 399, 449–451; b) M. Ishikawa, K. Maeda, Y. Mitsutsumi, E. Yashima, *J. Am. Chem. Soc.* **2004**, 126, 732–733; c) K. Maeda, K. Morino, Y. Okamoto, T. Sato, E. Yashima, *J. Am. Chem. Soc.* **2004**, 126, 4329–4342; d) T. Miyagawa, A. Furusho, K. Maeda, H. Katagari, Y. Furusho, E. Yashima, *J. Am. Chem. Soc.* **2005**, 127, 5018–5019; for supramolecular chiral memory effect, see: e) Y. Furusho, T. Kimura, Y. Mizuno, T. Aida, *J. Am. Chem. Soc.* **1997**, 119, 5267–5268; f) T. Mizuno, M. Takeuchi, I. Hamachi, K. Nakashima, S. Shinkai, *J. Chem. Soc. Perkin Trans. 2* **1998**, 2281–2288; g) L. J. Prins, F. de Jong, P. Timmerman, D. N. Reinhoudt, *Nature* **2000**, 408, 181–184; h) Y. Kubo, T. Ohno, J. Yamanaka, T. Tokita, T. Iida, Y. Ishimaru, *J. Am. Chem. Soc.* **2001**, 123, 12700–12701; i) R. Lauceri, A. Raudino, L. M. Scolaro, N. Micali, R. Purrello, *J. Am. Chem. Soc.* **2002**, 124, 894–895; j) H. Onouchi, T. Miyagawa, K. Morino, E. Yashima,

- Angew. Chem.* **2006**, *118*, 2441–2444; *Angew. Chem. Int. Ed.* **2006**, *45*, 2381–2384; k) T. Miyagawa, M. Yamamoto, R. Muraki, H. Onouchi, E. Yashima, *J. Am. Chem. Soc.* **2007**, *129*, 3676–3682.
- [8] a) H. Kusuyama, M. Takase, Y. Higashihara, H.-T. Tseng, Y. Chatani, H. Tadokoro, *Polymer* **1982**, *23*, 1256–1258; b) H. Kusuyama, N. Miyamoto, Y. Chatani, H. Tadokoro, *Polymer* **1983**, *24*, 119–122.
- [9] The st- and it-PMMA were synthesized using the stereospecific polymerization technique (see the Supporting Information). The number-average molecular weights ( $M_n$ ) and stereoregularities ( $mm/mr/rr$ ) were as follows: st-PMMA:  $M_n = 544\,000$  and  $mm/mr/rr = 0.6:94$ ; it-PMMA:  $M_n = 21\,800$  and  $mm/mr/rr = 97:3:0$ , in which  $m$  and  $r$  represent the it and st dyads of the meso and racemo sequences, respectively, and  $mm$ ,  $mr$ , and  $rr$  are the corresponding triad sequences.
- [10] K. Buyse, H. Berghmans, M. Bosco, S. Paoletti, *Macromolecules* **1998**, *31*, 9224–9230.
- [11] In the TEM observations, low doses and short exposure times were carefully applied to minimize any electron beam damage, but the st-PMMA chains were damaged, resulting in release of the encapsulated  $C_{60}$  molecules from the st-PMMA nanotubes, and a uniform and long 1D array of  $C_{60}$  molecules, as expected from the AFM image (Figure 3a), could not be observed; see Figure S7 in the Supporting Information for more details of the TEM observations.
- [12] J. Kumaki, T. Kawauchi, K. Okoshi, H. Kusanagi, E. Yashima, *Angew. Chem.* **2007**, *119*, 5444–5447; *Angew. Chem. Int. Ed.* **2007**, *46*, 5348–5351.
- [13] A macromolecular conformational change driven by chiral solvation was reported: M. M. Green, C. Khatri, N. C. Peterson, *J. Am. Chem. Soc.* **1993**, *115*, 4941–4942.
- [14] The gelation of st-PMMA ( $10\text{ mg mL}^{-1}$ ) slowly took place in 10 vol% **1** in toluene after 3 h, but the solution did not turn into a gel in 20 vol% **1**. In contrast, the gelation kinetics were accelerated in the presence of  $C_{60}$ , and the st-PMMA/ $C_{60}$  solution formed a gel in 10 and 20 vol% **1** after 10 min and 15 h, respectively (Table S3 in the Supporting Information).
- [15] Recently, Sanders and co-workers reported a one-dimensional helical array of  $C_{60}$  in self-assembled helical nanotubes: G. D. Pantoş, J.-L. Wietor, J. K. M. Sanders, *Angew. Chem.* **2007**, *119*, 2288–2290; *Angew. Chem. Int. Ed.* **2007**, *46*, 2238–2240.
- [16] F. Diederich, J. Effing, U. Jonas, L. Jullien, T. Plesniviy, H. Ringsdoef, C. Thilgen, D. Weinstein, *Angew. Chem.* **1992**, *104*, 1683–1686; *Angew. Chem. Int. Ed. Engl.* **1992**, *31*, 1599–1602.